AGU100 ADVANCING EARTH AND SPACE SCIENCE

Geophysical Research Letters

RESEARCH LETTER
10.1029/2018GL077901

Key Points:
- The liquid freshwater content in the Beaufort Gyre reaches a record high
- It is triggered by the concurrence of an anticyclonic wind regime and high freshwater availability
- The sea ice decline supplies meltwater and other freshwater as well to the Beaufort Gyre

Supporting Information:
- Supporting Information S1

Correspondence to:
Q. Wang,
Qiang.Wang@awi.de

Citation:
Wang, Q., Wekerle, C., Danilov, S., Koldunov, N., Sidorenko, D., Sein, D., et al. (2018). Arctic sea ice decline significantly contributed to the unprecedented liquid freshwater accumulation in the Beaufort Gyre of the Arctic Ocean. *Geophysical Research Letters*, *45*, 4956–4964. https://doi.org/10.1029/2018GL077901

Received 30 JAN 2018
Accepted 2 MAY 2018
Accepted article online 11 MAY 2018
Published online 23 MAY 2018

Arctic Sea Ice Decline Significantly Contributed to the Unprecedented Liquid Freshwater Accumulation in the Beaufort Gyre of the Arctic Ocean

Qiang Wang[1,2], Claudia Wekerle[1], Sergey Danilov[1,3], Nikolay Koldunov[1,4], Dmitry Sidorenko[1], Dmitry Sein[1,5], Benjamin Rabe[1], and Thomas Jung[1,6]

[1]Alfred Wegener Institute, Helmholtz Centre for Polar and Marine Research, Bremerhaven, Germany, [2]Laboratory for Regional Oceanography and Numerical Modeling, Qingdao National Laboratory for Marine Science and Technology, Qingdao, China, [3]Department of Mathematics and Logistics, Jacobs University, Bremen, Germany, [4]MARUM-Center for Marine Environmental Sciences, Bremen, Germany, [5]Shirshov Institute of Oceanology, Russian Academy of Science, Moscow, Russia, [6]Institute of Environmental Physics, University of Bremen, Bremen, Germany

Abstract The Beaufort Gyre (BG) is the largest liquid freshwater reservoir of the Arctic Ocean. The liquid freshwater content (FWC) significantly increased in the BG in the 2000s during an anticyclonic wind regime and remained at a high level despite a transition to a more cyclonic state in the early 2010s. It is not well understood to what extent the rapid sea ice decline during this period has modified the trend and variability of the BG liquid FWC in the past decade. Our numerical simulations show that about 50% of the liquid freshwater accumulated in the BG in the 2000s can be explained by the sea ice decline caused by the Arctic atmospheric warming. Among this part of the FWC increase, 60% can be attributed to surface freshening associated with the reduction of the net sea ice thermodynamic growth rate, and 40% to changes in ocean circulation, which makes freshwater more accessible to the BG for storage. Thus, the rapid increase of the BG FWC in the 2000s was due to the concurrence of the anticyclonic wind regime and the high freshwater availability. We also find that if the Arctic sea ice had not declined, the liquid FWC in the BG would have shown a stronger decreasing tendency at the beginning of the 2010s owing to the cyclonic wind regime. From our results we argue that changes in sea ice conditions should be adequately taken into account when it comes to understanding and predicting variations of BG liquid FWC in a changing climate.

Plain Language Summary Arctic Ocean is undergoing unprecedented changes, with significant accumulation of liquid freshwater. If the accumulated freshwater in the Arctic Ocean is released to the North Atlantic, it might significantly influence the large-scale ocean circulation and climate through its impact on deep water formation. The Beaufort Gyre (BG) is the Arctic Ocean's largest liquid freshwater reservoir. Its liquid freshwater content (FWC) increased significantly in the 2000s. At the same time Arctic sea ice has declined rapidly. A crucial question needs to be answered: To what extent the sea ice decline has modified the trend and variability of the BG liquid FWC? Our numerical simulations show that about 50% of the liquid freshwater accumulated in the BG in the 2000s can be explained by sea ice decline. Among this part of the FWC increase, 60% can be attributed to surface freshening associated with the reduction of the net sea ice thermodynamic growth rate, and 40% is due to changes in ocean circulation, which helped advect freshwater to the BG. From our results we argue that changes in sea ice conditions should be adequately taken into account when it comes to understanding and predicting variations of Arctic FWC in a changing climate.

1. Introduction

The Arctic air temperature has been increasing more strongly than the global mean (a phenomenon called Arctic amplification, e.g., Serreze & Barry, 2011). In the meantime the Arctic Ocean is undergoing unprecedented changes, with significant sea ice decline (Kwok et al., 2009; Laxon et al., 2013; Stroeve et al., 2012) and accumulation of liquid freshwater (Giles et al., 2012; Haine et al., 2015; McPhee et al., 2009; Polyakov et al., 2013; Proshutinsky et al., 2009; Rabe et al., 2014). If the accumulated freshwater in the Arctic Ocean will be released to the North Atlantic, it might significantly influence the large-scale ocean circulation and climate through its impact on deep water formation (Aagaard et al., 1985; Arzel et al., 2008).

The atmospheric Beaufort high-pressure system drives the anticyclonic Beaufort Gyre (BG) ocean circulation, making the BG region the Arctic Ocean's largest liquid freshwater reservoir. When the anticyclonic wind over the BG intensifies, freshwater accumulates through Ekman convergence and subsequent downwelling (anticyclonic regime); when the anticyclonic wind weakens or even changes to be cyclonic, freshwater is released through Ekman divergence and upwelling (cyclonic regime, Proshutinsky et al., 2002, 2009). The two regimes of BG circulation have alternated on multiyear time scales and led to the associated variability of BG freshwater content (FWC; Proshutinsky et al., 2002). In the 2000s there was a very large increase in BG FWC during an extended period of anticyclonic winds over the BG (Proshutinsky et al., 2015; Rabe et al., 2014). Perhaps surprisingly, when the winds shifted to a cyclonic regime in the following years (from 2009 to 2012), the change in FWC was fairly small (Zhang et al., 2016).

Besides the variability of atmospheric circulation over the BG, other processes may also influence the BG liquid FWC. For example, it was suggested that surface freshening caused by sea ice decline (Krishfield et al., 2014; Yamamoto-Kawai et al., 2009) and changes in river runoff pathways (Morison et al., 2012) can increase freshwater storage in the BG and Canadian Basin. When sea ice declines, the changes in sea ice concentration and speedup of sea ice drift can modify the momentum transfer from the atmosphere to the ocean (Martin et al., 2014), thus possibly changing the ocean surface stress and consequently freshwater storage.

While previous studies have significantly improved the knowledge of the BG dynamics, the extent to which the ongoing Arctic atmospheric warming is modifying the BG liquid FWC is not well understood yet. Sea ice decline in a changing climate can interplay with the effect of surface wind, thus modifying the response of BG freshwater storage to changes in the atmospheric circulation regime. Specifically, when the BG liquid FWC strongly increased in the 2000s and varied very modestly at the beginning of the 2010s, there was a pronounced decline in Arctic sea ice. This raises a crucial question: To what extent has the sea ice decline contributed to the liquid FWC increase in the BG?

In this paper we use numerical simulations to answer this question. We compare a model simulation in which the sea ice decline is removed by employing climatological air temperature and downward radiation fluxes against a hindcast simulation that is capable of reproducing the observed salinity changes and FWC variability in the BG region. Our results indicate that the sea ice decline has significantly contributed to both the recent increase and the subsequent, short-term stabilization of the BG liquid FWC. We conclude that the impact of the sea ice decline must be adequately taken into account while attempting to understand and predict variations of BG liquid FWC in a changing climate.

2. Model Description

We use the global Finite Element Sea ice-Ocean Model (FESOM) (Danilov et al., 2004; Timmermann et al., 2009; Wang et al., 2008), which is an ocean general circulation model with both the ocean and sea ice components using variable resolution unstructured meshes. Details of the latest stable model version are provided in Wang et al. (2014) and Danilov et al. (2015). The model has been applied in different Arctic Ocean studies (e.g., Wang et al., 2016, 2018; Wekerle, Wang, Danilov, et al., 2017; Wekerle, Wang, von Appen, et al., 2017). Only a brief description of the specific model configuration used in this work is given below.

The model grid has a nominal horizontal resolution of about 1° for most of the global ocean; north of 45°N the horizontal resolution is increased to 24 km and in the Arctic Ocean (defined by the Arctic gateways: Fram Strait, Barents Sea Opening, Bering Strait, and the Canadian Arctic Archipelago) the resolution is further refined to 4.5 km. In the vertical, 47 z levels are used with resolution of 10 m in the top 100 m and gradually decreased below the 100-m depth. Eddy parameterization is applied outside the Arctic region, where horizontal resolution is coarse. The eddy diffusivity is determined by considering local horizontal resolution (Wang et al., 2014).

The model is forced using atmospheric state variables from the JRA55 data set (Kobayashi et al., 2015), which has a spatial resolution of 0.55° and a temporal resolution of 3 hr. For the river runoff, data provided

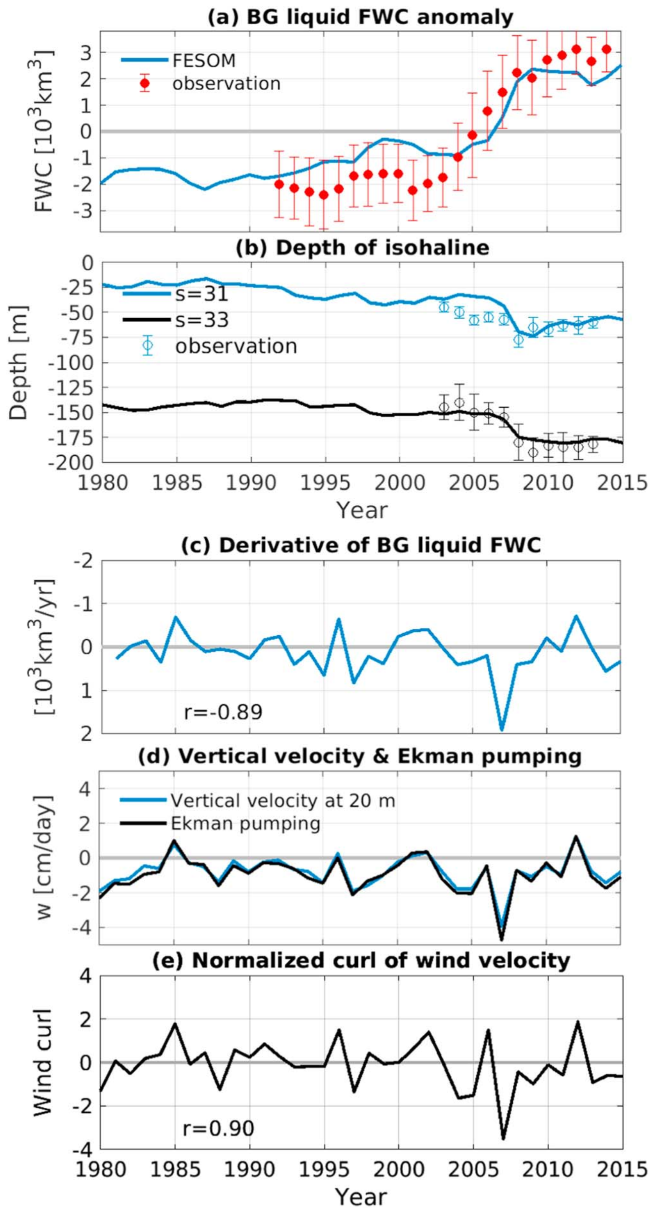

Figure 1. Results of the control simulation. (a) Anomaly of liquid freshwater content (FWC) in the Beaufort Gyre (BG) from the model simulation and observational data analysis. The observational estimate is described in Rabe et al. (2014). The BG region is indicated by the black box in Figure 4. (b) Depth of isohalines averaged in the central BG region (shown by the cyan box in Figure 4a); the observed changes in the depth of isohalines in this box are well reproduced in the model. The observation is described in Timmermans et al. (2014). (c) The time derivative of the BG liquid FWC; Its correlation with the Ekman pumping is −0.89 (significant at the 95% level). Note that the *y* axis is reversed. (d) Vertical velocity at 20 m and Ekman pumping averaged in the BG. (e) Curl of 10-m wind velocity averaged in the BG; Its correlation with the Ekman pumping is 0.90 (significant at the 95% level). *Annual mean* time series are shown; the same for time series in all other figures.

by the JRA55 repository are used. A hindcast simulation is carried out for the period 1958 to 2015 (called "control" hereafter). A sensitivity experiment representing a case without atmospheric warming in the Arctic is performed (called "climatology T&radiation"). In this simulation the climatology of near-surface air temperature and downward longwave and shortwave radiation (obtained by averaging the JRA55 data from 1971 to 2000 for each 3-hr segment) is used *over the Arctic region*, while all model settings and other forcing fields are the same as in control. This sensitivity experiment branches from control in 2001 and is run until 2015, covering the focus period of this study.

Two ocean passive tracers are introduced in the simulations to help interpret the model results. One is a freshwater tracer, which indicates the changes in ocean freshwater caused by the sea ice freezing and melting. The tracer is added to the model with zero initial values starting from 2001. It receives surface freshwater fluxes calculated using the sea ice thermodynamic growth rate (THDGR). (The sea ice THDGR [R, in m/s] is the rate of the change of sea ice thickness that corresponds to the transformation between liquid and solid water. It can be negative [melting] or positive [freezing] depending on the season. The passive tracer surface flux is defined as $F = -R(1 - S_{ice}/S_{ref})\rho_{ice}/\rho_{oce}$, where S_{ref} is the reference salinity used in the calculation of FWC, $S_{ice} = 4$ is the specified sea ice salinity in the model, and ρ_{ice} and ρ_{oce} are the specified sea ice and ocean reference density respectively.) From this tracer we can calculate the component of the liquid FWC change associated with the difference of the sea ice THDGR between the two simulations. Another passive tracer is meant to illustrate the change in the Pacific Water (PW) pathway. Initially, it is set to 0 in the ocean and starting from 1979 it is restored to 1 inside the Bering Strait.

3. Results

The control simulation shows a slight positive trend in the BG liquid FWC (FWC is calculated as $\int\int\int_D^0 (S_{ref} - S)/S_{ref}\,dxdydz$, where S is salinity, $S_{ref} = 34.8$ is the reference salinity, and D is the depth where salinity is equal to the reference salinity. In the paper we also discuss the freshwater inventory, which is the FWC *only integrated vertically*. It is defined as $\int_D^0 (S_{ref} - S)/S_{ref}\,dz$ and has unit m.) starting from the mid-1990s, followed by a rapid increase of the FWC in the second half of the 2000s, in agreement with the observational estimate (Figure 1a). After 2009 the rapid increase of FWC stops for a few years in the model. The $S = 31$ and $S = 33$ isohalines deepen consistently when the FWC increases, and the observed changes in the isohaline depths in the central BG are well reproduced in the model (Figure 1b).

The time derivative (i.e., the rate of the change) of the BG liquid FWC is highly correlated with the Ekman pumping over the BG (Figures 1c and 1d), while the variability of the Ekman pumping can be largely explained by the variation of atmospheric circulation regimes (as shown by the curl of near-surface wind velocity over the BG in Figure 1e). This demonstrates the dynamical relationship between BG liquid FWC and winds that has been established in previous studies (e.g., Proshutinsky et al., 2002, 2015). During the past two decades, the largest downwelling occurred in 2007, associated with a strong anticyclonic wind regime, and the most pronounced deepening of the isohalines and increase of the liquid FWC took place in 2007 and 2008. This is also consistent with previous model studies (Koldunov et al., 2014; Rabe et al., 2011; Zhang et al., 2016). In 2012 the Ekman pumping is positive (upward) due to cyclonic winds, and the FWC has a local minimum in 2013 before it starts to increase again.

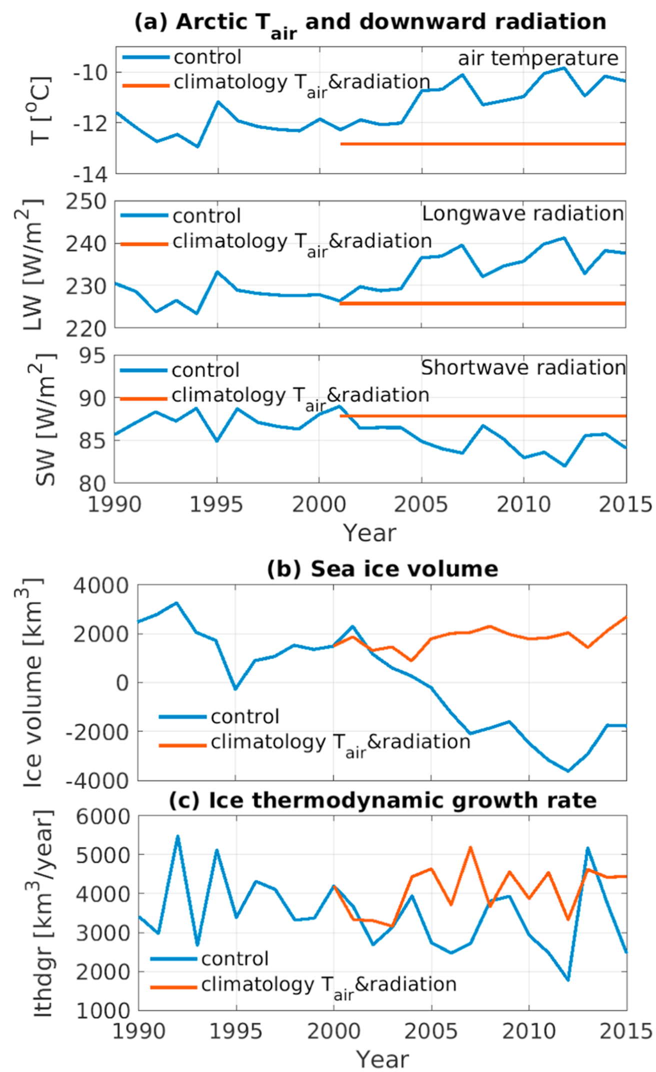

Figure 2. (a) Annual mean 10-m air temperature and longwave (LW) and shortwave (SW) radiation in the Arctic Ocean calculated from the atmospheric forcing data (JRA55) in the Arctic region of the ocean grid. Note that in both simulations the forcing temporal resolution is 3-hourly. (b) Arctic sea ice volume anomalies in the control and climatology T&radiation runs. (c) Sea ice thermodynamic growth rates averaged inside the Arctic Ocean.

The model also reproduces the observed declining trend of sea ice in the period 2001–2015 (supporting information Figure S1). Overall, the model is able to represent the critical aspects of observed recent Arctic climate changes. It provides a good basis for additional sensitivity experiments that help to shed light on the governing mechanisms of FWC changes.

In the sensitivity experiment climatology T&radiation, the near-surface air temperature and downward radiation fluxes in the Arctic region are kept at their climatological values, thereby effectively removing the Arctic atmospheric warming in the forcing (Figure 2a). The rapid Arctic sea ice decline is consequently eliminated in this experiment (Figure 2b), while some variability in the Arctic sea ice volume and THDGR is retained (Figures 2b and 2c), owing to variations in factors such as near-surface atmospheric winds. Atmospheric warming in the Arctic leads to a reduction in sea ice concentration and thickness (Figure S2) and speedup of sea ice drift (Figures S3a and S3b). The upper ocean circulation is also accordingly modified (Figure S3c). Previous observational and modeling studies have shown that Arctic sea ice is moving faster when sea ice declines (e.g., Kwok et al., 2013; Rampal et al., 2009; Zhang et al., 2012).

In climatology T&radiation the BG also accumulates freshwater from 2005 to 2009 but much less than in control (Figures 3a and 4a–4c). In this period, the BG liquid FWC increases by 3.21×10^3 km^3 in control, while the increase in climatology T&radiation is 1.54×10^3 km^3, only about 50% of that in control. Therefore, the Arctic atmospheric warming accounts for about 50% of the BG freshwater accumulation in this period. Integrated in the BG region, the equivalent FWC associated with salinity changes linked to the sea ice THDGR in control is 0.98×10^3 km^3 more than in climatology T&radiation until the end of 2009, while the difference of the total BG liquid FWC between the two simulations is 1.67×10^3 km^3 (Figure 3b). This means that the reduction in the net sea ice THDGR supplies 60% of the freshwater increase caused by the Arctic atmospheric warming in the 2000s.

In both simulations the time derivative of the BG liquid FWC is highly correlated with the Ekman pumping (Figures 3c and 3d); this indicates that the variability of Ekman pumping associated with the atmospheric circulation is the main dynamical driver of the variability of the BG liquid FWC, independent of the ongoing changes of the sea ice state. Our analysis shows that the difference of Ekman pumping between the two simulations is typically small in magnitude and very nonuniform in space, although the sea ice decline tends to enhance the ocean surface stress (Figure S4). The Ekman pumping averaged over the BG is nearly the same in the two simulations (Figure 3d). Therefore, the aforementioned significant FWC increase is not due to changes in local Ekman pumping in the BG region.

As mentioned above, 60% of the BG FWC difference between the two simulations is attributed to salinity changes associated with the lower net sea ice THDGR in control. Because the Ekman pumping averaged over the BG does not change between the two simulations, the remaining 40% of the FWC difference can only be explained by changes in pathways of other freshwater masses, that is, by the increased accessibility of freshwater to the BG for storage. The PW passive tracer released at the Bering Strait can be used as an example to illustrate that the ocean circulation pathways are indeed modified by the sea ice decline (Figure S5). We found that the amount of PW inflow through the Bering Strait is nearly the same in the two simulations (not shown). More PW is advected toward the BG from the north in the control simulation, which clearly indicates the occurrence of changes in the ocean circulation and water mass pathways.

From 2009 to 2012 the BG liquid FWC stops increasing in control (with a small decrease of 110 km^3 in this period), whereas it has a clear decreasing trend in climatology T&radiation (with a decrease of 460 km^3, Figure 3a). This indicates that, without the Arctic atmospheric warming, the BG FWC would have been more

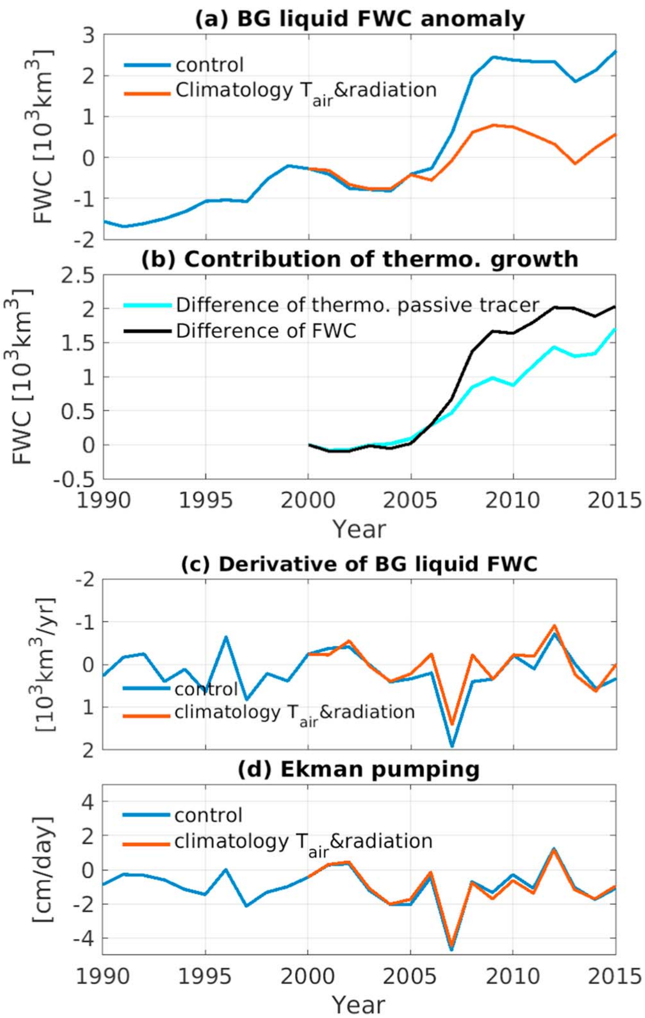

Figure 3. (a) Liquid freshwater content (FWC) in the Beaufort Gyre (BG). (b) The difference of liquid FWC in BG between the control and climatology T&radiation runs (black curve) and the difference of freshwater associated with the difference of the net sea ice thermodynamic growth rate between the two runs (cyan curve). (c) The time derivative of the BG liquid FWC. Note that the *y* axis is reversed. (d) Ekman pumping averaged in the BG.

strongly decreasing in this period. The Ekman pumping over the BG is the same between the two simulations in this period too (Figure 3d), and the difference in the BG FWC is mainly due to salinity changes associated with the difference in the net sea ice THDGR (as indicated by the very similar variation of the two curves after 2009 in Figure 3b). After the local minimum in 2013 the FWC starts to increase with a similar rate in the simulations.

4. Discussion

4.1. Contribution of Surface Freshening Induced by Net Sea Ice Melting

The liquid freshwater accumulation in the BG in the period 2005–2009 is higher in control not only in the upper ocean but also below 100-m depth (Figures 4c–4e). The reduction of the net sea ice THDGR freshens mainly the upper 100-m ocean, so the difference of the FWC in the upper 100 m between the two simulations spatially coincides with the FWC contribution associated with the difference of the net sea ice THDGR (Figures 4e and 4f).

The net sea ice THDGR is much lower in control than in climatology T&radiation in the northern Chukchi Sea (Figure S6), while the pronounced difference of the equivalent FWC associated with the sea ice THDGR is not found in this region, but rather inside the BG (Figure 4f). This indicates that the surface freshening due to the reduction of the net sea ice THDGR outside the BG region has significantly contributed to the increase of the BG liquid FWC.

A comment on the impact of other surface freshwater fluxes is given below. The ocean evaporation rate is not a specified surface forcing field in the simulations but is calculated during the model run time as in typical ocean-ice models. Because of larger open ocean area in control, the evaporation is accordingly larger (Figures S6c and S6d). The difference in the evaporation between the two simulations is relatively small, less than 5% of the difference of the net sea ice THDGR when averaged over the Amerasian part of the Arctic Ocean. This small change in the freshwater budget does not influence the main findings of this study, although the role of evaporation for the Arctic FWC change might become more important in a warmer climate in the future. Precipitation and river runoff remain the same in the two runs, so they do not lead to additional changes in the freshwater budget between the runs, even though they have interannual variability. However, their spatial distribution can be influenced by the ocean circulation (e.g., Morison et al., 2012; Yamamoto-Kawai et al., 2009), which can contribute to the change of the BG FWC (see further discussions below).

4.2. Dynamical Impact of Sea Ice Decline

The simulations indicate that the dynamical impact of the Arctic atmospheric warming is very important for the accumulation of freshwater in the BG. About 40% of the FWC difference between the two simulations cannot be directly attributed to ocean freshening associated with the reduction of the net sea ice THDGR. Because the Ekman pumping over the BG does not significantly change between the runs (Figures 3d and S4), this part of the FWC increase can only be attributed to the variation of ocean circulation and freshwater pathways outside the BG, which makes different freshwater masses more accessible to the BG for storage.

The only difference in the model configurations between the two runs is the thermal forcing over the Arctic Ocean (in terms of air temperature and downward radiation), and the dynamical impact mentioned above should be accordingly attributed to it. The Arctic atmospheric warming not only causes sea ice decline but also slightly increases the temperature in the halocline below the mixed layer in the Amerasian and Eurasian Basins

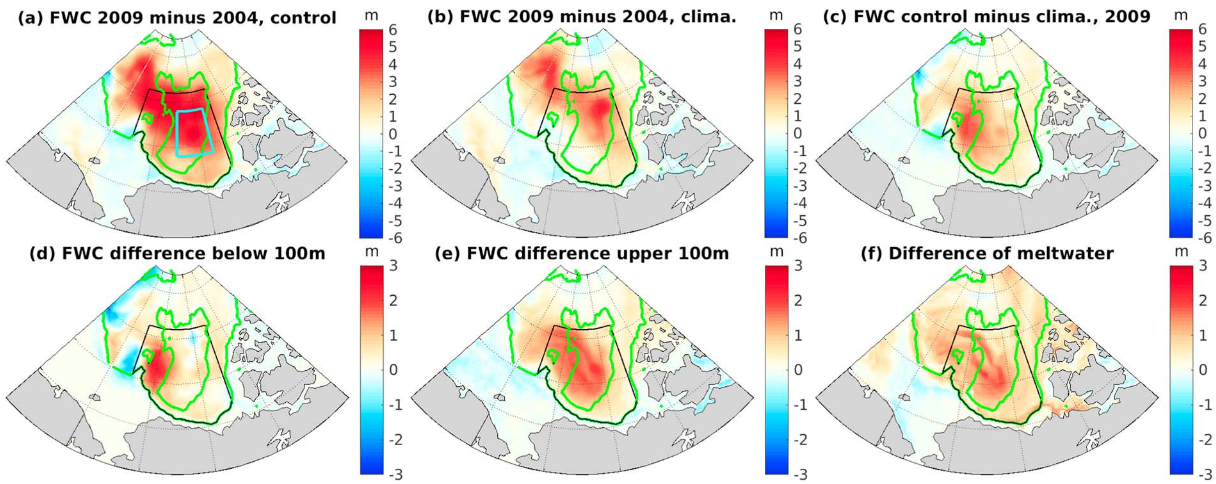

Figure 4. Difference of *vertically integrated* freshwater content (FWC, in m) between 2009 and 2004 in the (a) control and (b) climatology T&radiation runs. (c) Difference of FWC between the two runs in 2009; the components below 100 and above 100 m are shown in (d) and (e), respectively. (f) The difference of equivalent FWC associated with the difference of the net sea ice thermodynamic growth rate between the two simulations in 2009. The green contour lines indicate the 500- and 3,500-m isobaths. The black box indicates the BG region, and the cyan box in (a) indicates the central BG region.

(by less than 0.1°C). The salinity difference between the two runs (up to 0.4 averaged in the depth range of 50–150 m and even larger in the surface layer) is much more significant in terms of its contribution to changes in ocean density. Therefore, the sea ice decline is the direct cause of the changes in the upper ocean circulation through modifying ocean surface stress and ocean density, and we can attribute the difference of the BG liquid FWC between the two runs discussed above to the *sea ice decline*.

The impact of sea ice decline on the BG liquid FWC in the 2000s revealed by our simulations is summarized as follows. The Ekman convergence and downwelling associated with the anticyclonic wind regime acts to accumulate freshwater in the BG, while the sea ice decline further increases the BG liquid FWC by increasing the availability of freshwater: On the one hand, the sea ice decline decreases the ocean salinity through the reduction of the net sea ice THDGR; on the other hand, it makes freshwater more accessible to the BG by changing the ocean circulation and freshwater pathways outside the BG.

4.3. Implication for Predictability of BG Liquid FWC

Previous studies imply a certain predictability of the BG liquid FWC owing to its relationship with the wind forcing (Marshall et al., 2017). However, the significant impact of sea ice decline on the storage of freshwater in the BG might constitute a challenge for predicting the BG liquid FWC in a changing climate. One particular question is, if we know the atmospheric circulation, how well can we quantitatively predict the FWC? We carried out another three short sensitivity experiments (5 years each, named as shifted-wind-control). They branch off from control in 1991, 2001, and 2011, respectively, and are the same as the control run except that the wind field of the period 2005–2009 is used instead.

The wind in this period is in an outstanding anticyclonic regime. It turned out that the FWC in the BG tends to increase in all three sensitivity runs (Figures 5a and 5b), as expected from the regime of applied wind (indicated by the Ekman pumping averaged over the BG, Figure S7). However, the amount of increased FWC is quite different (Figure 5b). This indicates that we may infer the tendency of the BG FWC by just knowing the wind, but we need to know the initial state of the ocean and changes of the sea ice if we attempt to quantify the changes of the FWC.

To isolate the effect of sea ice decline, we carried out another two sensitivity experiments (named as shifted-wind-climatology). They are the same as shifted-wind-control, except that they branch off from climatology T&radiation. As the contribution of sea ice loss is eliminated, the increase of the BG FWC is smaller than in shifted-wind-control (Figure 5). Although some noticeable difference in the BG FWC is still present between the shifted-wind-climatology simulations (Figure 5d), their spread is smaller than in the case when sea ice declines (cf. Figures 5b and 5d), implying that the potential to predict FWC variability from winds would be

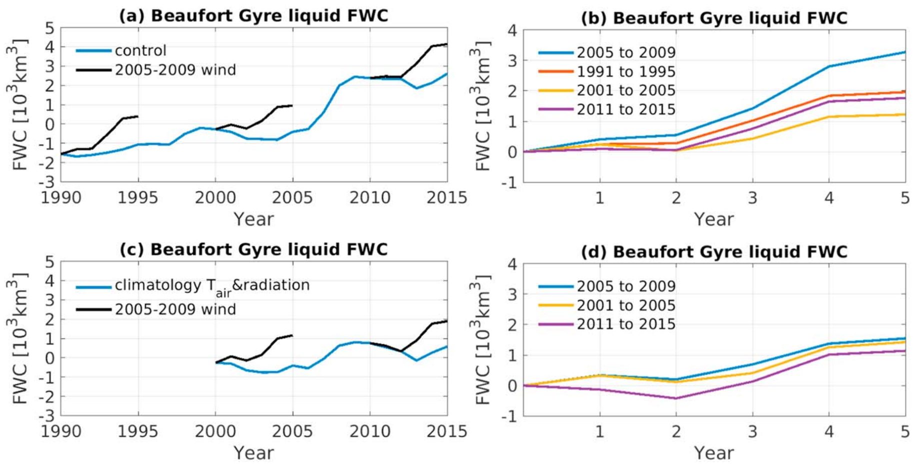

Figure 5. (a) Liquid freshwater content (FWC) anomaly in the Beaufort Gyre (BG) in the control simulation and three "shifted-wind-control" simulations. In the latter the wind field from 2005 to 2009 is used over the Arctic region. (b) The liquid FWC anomalies referenced to the corresponding initial FWC values, that is, the time series of the annual mean FWC minus the FWC value at the beginning of the corresponding simulation. (c, d) The same as (a) and (b) but for the climatology T&radiation and the shifted-wind-climatology simulations.

higher without sea ice loss caused by atmospheric warming. These sensitivity experiments also indicate that the initial conditions of the simulations can influence the evolution of the FWC, at least during the first few model years.

5. Conclusions

Due to the climate relevance of Arctic freshwater, better understanding the response of the BG liquid FWC to changes in wind regimes and sea ice conditions is high on the agenda of the Arctic research community. In this study we used numerical simulations to understand the impact of sea ice on the BG liquid FWC. We carried out a sensitivity experiment that is forced by climatological air temperature and downward radiation fluxes in the Arctic region to eliminate the sea ice decline. By comparing this simulation with a hindcast simulation that adequately represents the decline of sea ice and the variability of liquid FWC in the BG, we quantified the contribution of the Arctic sea ice decline to the increase of the BG liquid FWC in the 2000s and the subsequent short-term stabilization of the BG at the beginning of the 2010s.

With an anticyclonic wind regime in the late 2000s, the Ekman convergence and downwelling led to accumulation of liquid freshwater in the BG. The simulations reveal that the sea ice decline significantly enhanced the increase of BG FWC through both the surface freshening (due to the reduction of the net sea ice THDGR) and increasing the accessibility of other freshwater to the BG (due to the modification of upper ocean circulation and freshwater pathways). The simulations show that the BG FWC increases by 3, 210 km^3 between 2005 and 2009; about 50% of this increase (1, 670 km^3) can be attributed to the sea ice decline. Of this 1, 670 km^3 contribution, 980 km^3 (60%) results directly from the surface freshening caused by the reduction of the net sea ice THDGR. The other 40% is attributed to other freshwater that becomes accessible to the BG due to the change of the ocean circulation, arguably mainly caused by the sea ice decline. Overall, the concurrence of the anticyclonic wind regime and the high freshwater availability provided a favorable condition for freshwater to accumulate in the BG in the 2000s.

After 2009, the wind regime became cyclonic, and the BG liquid FWC stopped increasing for a few years. Our simulations reveal that if there were no sea ice decline, the BG FWC would have shown a strong decreasing tendency. In other words, the sea ice decline helped to maintain the high level of the FWC at the beginning of the 2010s. In this period, the difference of BG FWC between the two runs can be largely explained by salinity changes associated with the reduction of the net sea ice THDGR.

In general, numerical simulations have uncertainties. Although our hindcast simulation reasonably reproduces the critical aspects of observed Arctic climate changes, the quantitative findings can only be considered as a guideline for understanding the relative importance of different processes. Such process studies are particularly helpful since observational data are still sparse.

Our study suggests that the impact of sea ice loss should be properly taken into account when we want to better understand and predict the changes of the BG liquid FWC. Its impact on other parts of the Arctic Ocean will be investigated in future work.

Acknowledgments
We thank the two reviewers for their very helpful comments. This work was supported by the Helmholtz Climate Initiative REKLIM (Regional Climate Change), the FRAM (FRontiers in Arctic marine Monitoring) program, the project of the Collaborative Research Centre TRR 181 "Energy Transfer in Atmosphere and Ocean" funded by the German Research Foundation, the EC project PRIMAVERA, the state assignment of FASO Russia (theme 0149-2018-0014), and the NATMAP project in the framework of ERA-Net Plus with Russia funded by the German Federal Ministry for Education and Research. The model results can be found at a designated data center via swiftbrowser.dkrz.de/Wang/.The simulations were performed at the North-German Supercomputing Alliance (HLRN).

References

Aagaard, K., Swift, J. H., & Carmack, E. (1985). Thermohaline circulation in the Arctic mediterranean seas. *Journal of Geophysical Research*, *90*, 4833–4846.

Arzel, O., Fichefet, T., Goosse, H., & Dufresne, J.-L. (2008). Causes and impacts of changes in the Arctic freshwater budget during the 20th and 21st centuries in an AOGCM. *Climate Dynamics*, *30*, 37–58.

Danilov, S., Kivman, G., & Schröter, J. (2004). A finite-element ocean model: Principles and evaluation. *Ocean Modelling*, *6*, 125–150.

Danilov, S., Wang, Q., Timmermann, R., Iakovlev, N., Sidorenko, D., Kimmritz, M., et al. (2015). Finite-element sea ice model (FESIM), version 2. *Geoscientific Model Development*, *8*, 1747–1761.

Giles, K. A., Laxon, S. W., Ridout, A. L., Wingham, D. J., & Bacon, S. (2012). Western Arctic Ocean freshwater storage increased by wind-driven spin-up of the Beaufort Gyre. *Nature Geoscience*, *5*, 194–197.

Haine, T., Curry, B., Gerdes, R., Hansen, E., Karcher, M., Lee, C., et al. (2015). Arctic freshwater export: Status, mechanisms, and prospects. *Global and Planetary Change*, *125*, 13–35.

Kobayashi, S., Ota, Y., Harada, Y., Ebita, A., Moriya, M., Onoda, H., et al. (2015). The JRA-55 reanalysis: General specifications and basic characteristics. *Journal of the Meteorological Society of Japan*, *95*, 5–48.

Koldunov, N. V., Serra, N., Köhl, A., Stammer, D., Henry, O., Prandi, P., et al. (2014). Multimodel simulations of Arctic Ocean sea surface height variability in the period 1970–2009. *Journal of Geophysical Research: Oceans*, *119*, 8936–8954. https://doi.org/10.1002/2014JC010170

Krishfield, R. A., Proshutinsky, A., Tateyama, K., Williams, W. J., Carmack, E. C., McLaughlin, F. A., & Timmermans, M. L. (2014). Deterioration of perennial sea ice in the Beaufort Gyre from 2003 to 2012 and its impact on the oceanic freshwater cycle. *Journal of Geophysical Research: Oceans*, *119*, 1271–1305. https://doi.org/10.1002/2013JC008999

Kwok, R., Cunningham, G. F., Wensnahan, M., Rigor, I., Zwally, H. J., & Yi, D. (2009). Thinning and volume loss of the Arctic Ocean sea ice cover: 2003–2008. *Journal of Geophysical Research*, *114*, C07005. https://doi.org/10.1029/2009JC005312

Kwok, R., Spreen, G., & Pang, S. (2013). Arctic sea ice circulation and drift speed: Decadal trends and ocean currents. *Journal of Geophysical Research: Oceans*, *118*, 2408–2425. https://doi.org/10.1002/jgrc.20191

Laxon, S. W., Giles, K. A., Ridout, A. L., Wingham, D. J., Willatt, R., Cullen, R., et al. (2013). CryoSat-2 estimates of Arctic sea ice thickness and volume. *Geophysical Research Letters*, *40*, 732–737. https://doi.org/10.1002/grl.50193

Marshall, J., Scott, J., & Proshutinsky, A. (2017). "Climate response functions" for the Arctic Ocean: A proposed coordinated modelling experiment. *Geoscientific Model Development*, *10*, 2833–2848.

Martin, T., Steele, M., & Zhang, J. (2014). Seasonality and long-term trend of Arctic Ocean surface stress in a model. *Journal of Geophysical Research: Oceans*, *119*, 1723–1738. https://doi.org/10.1002/2013JC009425

McPhee, M. G., Proshutinsky, A., Morison, J. H., Steele, M., & Alkire, M. B. (2009). Rapid change in freshwater content of the Arctic Ocean. *Geophysical Research Letters*, *36*, L10602. https://doi.org/10.1029/2009GL037525

Morison, J., Kwok, R., Peralta-Ferriz, C., Alkire, M., Rigor, I., Andersen, R., & Steele, M. (2012). Changing Arctic Ocean freshwater pathways. *Nature*, *481*, 66–70.

Polyakov, I. V., Bhatt, U. S., Walsh, J. E., Abrahamsen, E. P., Pnyushkov, A. V., & Wassmann, P. F. (2013). Recent oceanic changes in the Arctic in the context of long-term observations. *Ecological Applications*, *23*, 1745–1764.

Proshutinsky, A., Bourke, R. H., & McLaughlin, F. A. (2002). The role of the Beaufort Gyre in Arctic climate variability: Seasonal to decadal climate scales. *Geophysical Research Letters*, *29*, 2100. https://doi.org/10.1029/2002GL015847

Proshutinsky, A., Dukhovskoy, D., Timmermans, M.-L., Krishfield, R., & Bamber, J. L. (2015). Arctic circulation regimes. *Philosophical Transactions of the Royal Society A*, *373*, 20140160.

Proshutinsky, A., Krishfield, R., Timmermans, M.-L., Toole, J., Carmack, E., McLaughlin, F., et al. (2009). Beaufort Gyre freshwater reservoir: State and variability from observations. *Journal of Geophysical Research*, *114*, C00A10. https://doi.org/10.1029/2008JC005104

Rabe, B., Karcher, M., Kauker, F., Schauer, U., Toole, J. M., Krishfield, R. A., et al. (2014). Arctic ocean basin liquid freshwater storage trend 1992–2012. *Geophysical Research Letters*, *41*, 961–968. https://doi.org/10.1002/2013GL058121

Rabe, B., Karcher, M., Schauer, U., Toole, J. M., Krishfield, R. A., Pisarev, S., et al. (2011). Assessment of Arctic Ocean freshwater content changes from the 1990s to the 2006–2008 period. *Deep-sea Research Part I-Oceanographic Research Papers*, *58*, 173–185.

Rampal, P., Weiss, J., & Marsan, D. (2009). Positive trend in the mean speed and deformation rate of Arctic sea ice, 1979–2007. *Journal of Geophysical Research*, *114*, C05013. https://doi.org/10.1029/2008JC005066

Serreze, M. C., & Barry, R. G. (2011). Processes and impacts of Arctic amplification: A research synthesis. *Global and Planetary Change*, *77*, 85–96.

Stroeve, J. C., Kattsov, V., Barrett, A., Serreze, M., Pavlova, T., Holland, M., & Meier, W. N. (2012). Trends in Arctic sea ice extent from CMIP5, CMIP3 and observations. *Geophysical Research Letters*, *39*, L16502. https://doi.org/10.1029/2012GL052676

Timmermann, R., Danilov, S., Schröter, J., Böning, C., Sidorenko, D., & Rollenhagen, K. (2009). Ocean circulation and sea ice distribution in a finite element global sea ice-ocean model. *Ocean Modelling*, *27*, 114–129.

Timmermans, M.-L., Proshutinsky, A., Golubeva, E., Jackson, J. M., Krishfield, R., McCall, M., et al. (2014). Mechanisms of Pacific Summer Water variability in the Arctic's Central Canada Basin. *Journal of Geophysical Research: Oceans*, *119*, 7523–7548. https://doi.org/10.1002/2014JC010273

Wang, Q., Danilov, S., Jung, T., Kaleschke, L., & Wernecke, A. (2016). Sea ice leads in the Arctic Ocean: Model assessment, interannual variability and trends. *Geophysical Research Letters*, *43*, 7019–7027. https://doi.org/10.1002/2016GL068696

Wang, Q., Danilov, S., & Schröter, J. (2008). Finite element ocean circulation model based on triangular prismatic elements, with application in studying the effect of vertical discretization. *Journal of Geophysical Research*, *113*, C05015. https://doi.org/10.1029/2007JC004482

Wang, Q., Danilov, S., Sidorenko, D., Timmermann, R., Wekerle, C., Wang, X., et al. (2014). The Finite Element Sea Ice-Ocean Model (FESOM) v.1.4: Formulation of an ocean general circulation model. *Geoscientific Model Development*, *7*, 663–693.

Wang, Q., Wekerle, C., Danilov, S., Wang, X., & Jung, T. (2018). A 4.5 km resolution Arctic Ocean simulation with the global multi-resolution model FESOM 1.4. *Geoscientific Model Development*, *11*, 1229–1255.

Wekerle, C., Wang, Q., Danilov, S., Schourup-Kristensen, V., von Appen, W.-J., & Jung, T. (2017). Atlantic Water in the Nordic Seas: Locally eddy-permitting ocean simulation in a global setup. *Journal of Geophysical Research: Oceans*, *122*, 914–940. https://doi.org/10.1002/2016JC012121

Wekerle, C., Wang, Q., von Appen, W.-J., Danilov, S., Schourup-Kristensen, V., & Jung, T. (2017). Eddy-resolving simulation of the Atlantic Water circulation in the Fram Strait with focus on the seasonal cycle. *Journal of Geophysical Research: Oceans*, *122*, 8385–8405. https://doi.org/10.1002/2017JC012974

Yamamoto-Kawai, M., McLaughlin, F. A., Carmack, E. C., Nishino, S., Shimada, K., & Kurita, N. (2009). Surface freshening of the Canada Basin, 2003–2007: River runoff versus sea ice meltwater. *Journal of Geophysical Research*, *114*, C00A05. https://doi.org/10.1029/2008JC005000

Zhang, J., Lindsay, R., Schweiger, A., & Rigor, I. (2012). Recent changes in the dynamic properties of declining Arctic sea ice: A model study. *Geophysical Research Letters*, *39*, L20503. https://doi.org/10.1029/2012GL053545

Zhang, J., Steele, M., Runciman, K., Dewey, S., Morison, J., Lee, C., et al. (2016). The Beaufort Gyre intensification and stabilization: A model-observation synthesis. *Journal of Geophysical Research: Oceans*, *121*, 7933–7952. https://doi.org/10.1002/2016JC012196